Intermediates in the Ferrous Oxidase Cycle of Bleomycin[†]

William J. Caspary,* D. Allen Lanzo, and Craig Niziak

ABSTRACT: We have previously shown that the bleomycin-induced autoxidation of ferrous iron follows Michaelis–Menten kinetics which are characteristic of enzymatic reactions [Caspary, W. J., Lanzo, D. A., Niziak, C., Friedman, R., & Bachur, N. R. (1979) *Mol. Pharmacol. 16*, 256]. In this paper, we identify the iron complexes formed during this reaction. The first is a ferrous iron–bleomycin complex which can be considered the catalyst substrate complex. The product of this reaction is a ferric iron–bleomycin complex which is found in a low-spin and a high-spin form. The relative concentrations of these two forms are a function of pH. Glutathione, a biologically relevant reducing agent, binds to the ferric iron–bleomycin complex, reduces it, and may serve as a model for the reduction of the ferric iron–bleomycin complex to the ferrous state during the catalytic cycle. Oxygen uptake induced by bleomycin and ferrous iron is not inhibited by superoxide dismutase (SOD) or catalase. In the absence of bleomycin, catalase strongly inhibits oxygen uptake. This suggests the presence of a relatively stable intermediate in which the superoxide radical is not readily accessible to superoxide dismutase. At pH 9.3, we are able to observe a transient species by electron spin resonance (ESR). When potassium superoxide is added to the ferric iron–bleomycin complex, the same ESR spectrum is produced. We suggest that a transient species composed of a ferric iron, the superoxide ion, and bleomycin is formed. The precise nature of the binding cannot be determined from the data presented.

The bleomycins are a family of glycopeptides produced by *Streptomyces verticillus* and are used clinically against various tumors. They were discovered by Umezawa (Umezawa et al., 1966a,b). Bleomycin A_2 (Figure 1) is the principal component of the clinical drug and possesses a molecular weight of approximately 1450.

The mechanism of the antitumor activity of bleomycin is unknown. It is known that bleomycin binds and breaks DNA (Suzuki et al., 1969; Takeshita et al., 1974, 1976; Iqbal et al., 1976; Kohn & Ewig, 1976; Haidle, 1971; Haidle et al., 1972; Kuo et al., 1973; Bearden & Haidle, 1975; Bearden et al., 1977; Lloyd et al., 1978). Ferrous iron and bleomycin, in the presence of reducing agents, stimulate DNA degradation, a process that may be involved in cell toxicity (Sausville et al., 1976, 1978a,b; Lown & Sim, 1977). This process causes oxygen reduction and the production of the superoxide ion and the hydroxyl radical, species that may play a role in this drug's ability to break DNA (Lown & Sim, 1977).

During our studies on the interaction of ferrous iron with bleomycin A_2, we observed that bleomycin A_2 stimulates a ferrous iron dependent consumption of oxygen. We observed that this consumption of oxygen follows classical Michaelis–Menten kinetics (Caspary et al., 1979) which are characteristic of enzymatic reactions. We suggested the scheme shown in Figure 2. In this paper, we present evidence for the iron intermediates of this reaction and identify a structure that appears to be composed of ferric iron, superoxide ion, and bleomycin.

We compared the superoxide radical with glutathione in their abilities to reduce the ferric iron–bleomycin complex. On the basis of these results, we suggest that the catalytic cycle we proposed for the reaction of bleomycin and iron can be oxidatively driven by oxygen and reductively driven by a cellular reducing agent.

Materials and Methods

Bleomycin A_2 was obtained from the Natural Products Branch, Division of Cancer Treatment, National Cancer Institute, National Institutes of Health. Purity was checked by thin-layer chromatography and by ^{13}C nuclear magnetic resonance spectroscopy. Ten microliters of a bleomycin A_2 solution (2.8 mg/mL) was spotted on a silica gel 60 plate (0.25 mm thickness, E. M. Laboratories, Inc.). The plate was chromatographed in 10% ammonium acetate–methanol (1:1) according to the method of Umezawa et al. (1966b). One spot was observed under shortwave UV light at 2537 Å. The R_f value was 0.33 [published value for bleomycin A_2 is 0.40 (Umezawa et al., 1966b)]. The ^{13}C nuclear magnetic resonance spectrum of bleomycin A_2 confirmed that any impurity, if present, was less than 1%. All peaks were assigned to bleomycin carbons (Naganawa et al., 1977). No extraneous peaks were present. Since the signal/noise was 120:1 and extraneous peaks would be observable at a signal/noise of 1:1, we concluded that our sample of bleomycin A_2 was essentially pure.

The oxygen content of reaction mixtures was measured with a Clark electrode in a Yellow Springs Model 53 instrument. Reaction mixtures (final volume 1 mL) contained 0.1 M sodium maleate buffer (pH 6.2), 10^{-5} M bleomycin A_2 (when used), and 5×10^{-4} M $FeSO_4$. Buffer and water were aerated by bubbling with air for 3 min at 37 °C. Bleomycin A_2 was added to the reaction vessel, the electrode was inserted, and the system was equilibrated for 1 min while being monitored for oxygen content. Fifty microliters of $FeSO_4$ (10^{-2} M) was injected into the reaction vessel, and the change in oxygen content was determined. $FeSO_4$ solutions were made fresh daily in water that had been sparged with N_2. Rates of oxygen consumption were calculated from the initial linear electrode response. The value used for the dissolved oxygen content in the reaction mixture was 0.16 mM.

Visible–UV spectra were obtained on a Cary 14 recording spectrophotometer. Succinate (0.1 M) rather than 0.1 M maleate was used because maleate posesses a UV band at 280 nm that interferes with the 288-nm peak of bleomycin A_2. Mixtures contained 4×10^{-4} M ferrous or ferric iron and 4×10^{-4} M bleomycin A_2.

[†] From the Baltimore Cancer Research Program, National Cancer Institute, National Institutes of Health, Baltimore, Maryland 21201. *Received November 1, 1979; revised manuscript received February 10, 1981.*

* Address correspondence to this author at the Cellular and Genetic Toxicology Branch, National Cancer Institute/National Toxicology Program, National Institutes of Health, Bethesda, MD 20205.

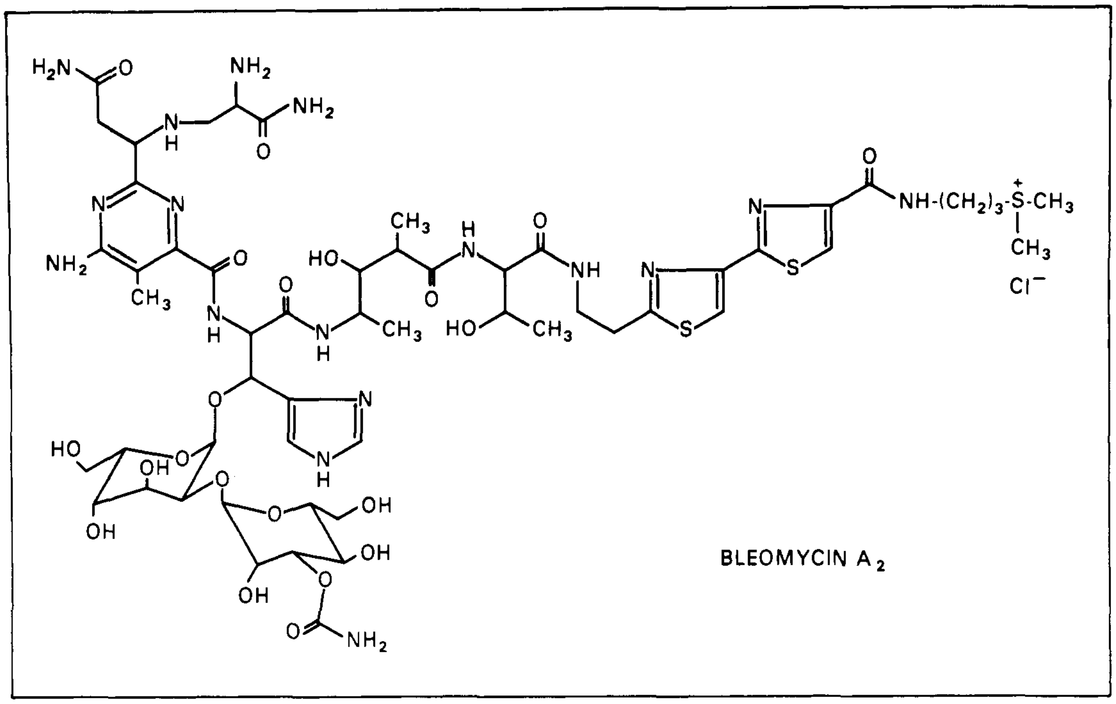

FIGURE 1: Chemical structure of bleomycin A_2.

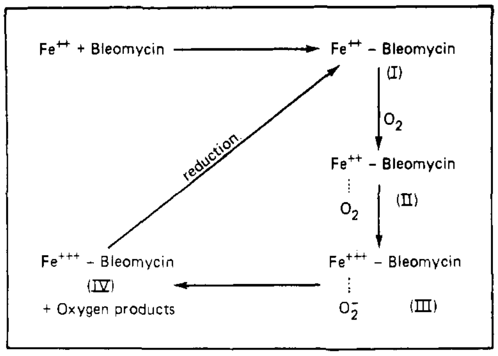

FIGURE 2: Proposed mechanism for the reaction of bleomycin, iron, and oxygen. Structures II and III are included to demonstrate a dynamic process whereby an electron is transferred from the ferrous to oxygen. The actual structure and binding characteristics of these species cannot be inferred from the data presented in this paper.

Electron spin resonance spectra of the iron–bleomycin complexes were obtained on a Varian E-109 ESR spectrometer. Integrations for concentrations were performed on a Nicolet 1180 computer. Solutions containing 6×10^{-3} M bleomycin and 10^{-4} M iron (ferrous or ferric) were prepared by adding 10 μL of 10^{-2} M ferrous or ferric iron in N_2-sparged water to 1 mL of an aerated solution of 6×10^{-3} M bleomycin. Excess bleomycin was used to ensure that all the iron was bound. Solutions were added to ESR tubes and frozen in liquid N_2. Spectra were obtained with samples at -178 °C (uncalibrated). Samples were prepared in 0.1 M glycine–HCl at pH 2.3, 0.1 M maleate at pH 6.2, and 0.1 M glycine–KOH at pH 9.3. Microwave power = 196 mW; modulation amplitude = 10 G. None of the ESR signals reported here saturated below 200 mW. Once it was determined that ESR spectra of ferric iron–bleomycin A_2 and ferric iron–blenoxane were identical, blenoxane was used for the ESR experiments. Blenoxane is the clinical preparation of bleomycin distributed by Bristol Laboratories and contains a mixture of bleomycins containing predominantly bleomycin A_2 and bleomycin B_2.

Results

Above pH 5, bleomycin A_2 stimulates a ferrous iron dependent consumption of oxygen (Table I). Although ferrous iron spontaneously autoxidizes to the ferric state, the addition of bleomycin A_2 accelerates the process. Preheating the bleomycin A_2 does not affect its ability to accelerate oxygen uptake. At pH 6.2 or 6.8 in maleate, the spontaneous rate of oxygen consumption is negligible (Table I). Phosphate, at a similar pH, produces a measurable rate of ferrous iron induced oxygen consumption. Increasing the pH increases the initial rates of spontaneous consumption of oxygen by ferrous iron but appears to have no significant effect on that induced by bleomycin, which is shown as the difference in induced rates in the presence and absence of bleomycin (Table I). Changes in phosphate or maleate concentrations between 1 mM and 0.1 M had little effect on the rates of oxygen consumption (data not shown).

Table I: pH Dependence of Bleomycin-Iron Induced Oxygen Uptake[a]

		μmol of O_2 utilized/min		
pH	buffer (0.1 M)	−bleomycin	+bleomycin	difference
2.3	glycine-HCl	0.00	0.00	0.00
3.0	glycine-HCl	0.00	0.00	0.00
4.0	acetate	0.00	0.00	0.00
5.0	acetate	0.00	0.06	0.06
5.6	acetate	0.00	0.19	0.19
6.0	phosphate	0.11	0.33	0.22
6.2	maleate	0.00	0.16	0.16
6.8	maleate	0.01	0.30	0.29
7.0	phosphate	0.28	0.39	0.11
7.5	Tris	0.13	0.29	0.16
8.0	phosphate	0.33	0.50	0.17
8.5	Tris	0.55	0.66	0.11
9.3	glycine-NaOH	0.32	0.48	0.16

[a] Oxygen uptake measurements were made as described under Materials and Methods; $FeSO_4$ (10^{-4} M) and 10^{-4} M bleomycin A_2 were used. The rates described are initial rates of oxygen utilization obtained by measuring the slope of the initial part of the oxygen uptake response.

Certain chelating agents such as 2,2′-bipyridine and *o*-phenanthroline significantly inhibit the induction of oxygen

Table II: Effect of Chelators and Enzymes on the Rate of Oxygen Uptake Induced by Iron and Bleomycin

bleomycin A_2	effectors	µmol of O_2 utilized/min
	A	
–		0.11
+		0.26
+	2,2′-bipyridine	0.00
+	*o*-phenanthroline	0.00
–	EDTA	1.00
+	EDTA	1.00
+	SOD	0.25
+	catalase	0.20
–	catalase	0.04
	B	
–		0.00
+		0.04
+	catalase	0.04

[a] Oxygen uptake measurements were made as described under Materials and Methods. The rates described are initial rates of oxygen utilization obtained by measuring the slope of the initial part of the oxygen uptake response. Maleate buffer (0.1 M), pH 6.2, and 5 × 10^{-4} M $FeSO_4$ (A) or 10^{-4} M $FeSO_4$ (B) were used. The concentration of bleomycin A_2 was 10^{-5} M. The concentrations of 2,2′-bipyridine and *o*-phenanthroline were 2 mM; the concentration of EDTA was 1 mM; SOD and catalase concentrations were 100 µg/mL. The effectors were added to the reaction mixture just before inserting the electrode.

uptake by bleomycin A_2 and ferrous iron (Table IIA). Ethylenediaminetetraacetic acid (EDTA), another chelating agent, stimulates the initial rate of oxygen uptake by ferrous iron; the presence of bleomycin appears to have no effect. Superoxide dismutase (SOD) had no effect on the observed rates in the presence of bleomycin A_2 (Table IIA), though in the absence of bleomycin, it strongly inhibits oxygen uptake. At concentrations of 5 × 10^{-4} M $FeSO_4$ and 10^{-5} M bleomycin, the effect of catalase is unclear. Since ferrous iron at this concentration has the ability to induce oxygen consumption at an initial rate of 0.11 µmol of O_2/min, the decrease in the rate of oxygen consumption observed in the presence of catalase could be explained by an inhibition of this spontaneous mechanism, assuming that this spontaneous mechanism is still significant in the presence of bleomycin. At 10^{-4} M ferrous iron, the spontaneous rate is 0 (Table IIB), and catalase has no inhibitory effect. In the presence of bleomycin, SOD and catalase have no effect on the initial rates of oxygen uptake. In the absence of bleomycin, catalase inhibits oxygen consumption.

The reduction of oxygen by ferrous iron and bleomycin is expected to produce the superoxide radical and hydrogen peroxide. To ensure that hydrogen peroxide is formed, we monitored the formation of ethylene from methional by gas chromatography (Beauchamp & Fridovich, 1970) and showed that its formation is inhibited by the addition of catalase. Incubation of ferrous iron in a 50 µM, aerobic tris(hydroxymethyl)aminomethane (Tris) buffered solution at pH 7.5 with methional resulted in a gas chromatographic peak with characteristics similar to that of pure ethylene. Cochromatographing standard ethylene with the gaseous products of ferrous iron autoxidation and methional produced one peak. The omission of ferrous iron, methional, or oxygen eliminated the production of ethylene. Catalase and ethanol inhibited ethylene production. The inhibition of ethylene production in the presence of bleomycin was larger than the inhibition in its absence. Thus, at least part of the catalase inhibition observed in the presence of bleomycin must be due to a bleomycin-induced mechanism.

The optical spectrum of the ferrous iron–bleomycin complex

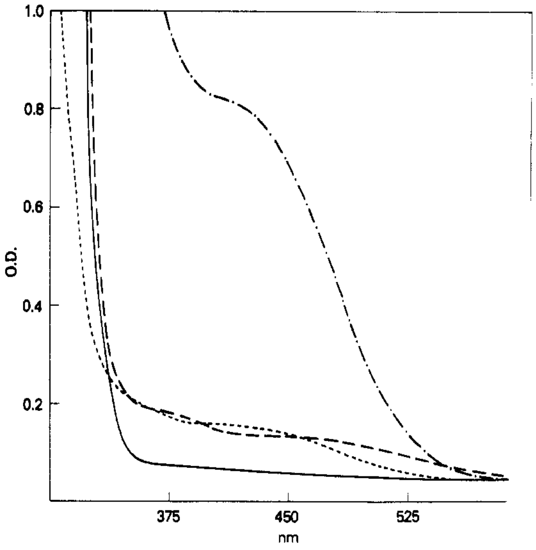

FIGURE 3: Visible–UV spectra of the ferrous iron–bleomycin and the ferric iron–bleomycin complexes. In one of these experiments, 4 × 10^{-4} M ferrous iron was placed in one cuvette and 4 × 10^{-4} M bleomycin in another. These were placed in tandem in a Cary 14 recording spectrophotometer and the additive spectrum (—) was recorded. When the two reactants were mixed in the same cuvette under nitrogen, the spectrum (– – –) was obtained. Addition of air to produce the ferric iron–bleomycin complex shifted the absorption bands from 375 and 460 nm to a band at 430 nm (- - -). Diluting this solution 7-fold gave rise to the spectrum indicated by (–•–•).
Sodium succinate (0.1 M), pH 6.2, was used in these experiments.

at pH 6.2 differed slightly from that observed previously (Sausville et al., 1978a). When carefully sparged with nitrogen at pH 6.2 in 0.1 M succinate, a solution of ferrous sulfate and bleomycin A_2 possesses a weak visible spectrum with a broad peak arount 460 nm and another at 375 nm (Figure 3). The addition of air produced an optical spectrum of greater intensity and a peak at 430 nm. When this aerated solution was diluted 7-fold, the intensity of the optical spectrum was similar to that formed initially under anaerobic conditions. The differences between the ferric and ferrous iron complexes are clearly seen (Figure 3). To ensure that the optical spectrum with peaks at 460 and 375 nm are due to a ferrous iron–bleomycin complex, we added a small amount of sodium dithionite to a nitrogen-sparged solution containing ferrous iron and bleomycin. No changes in the optical spectrum were observed (Sausville et al., 1978a,b). In contrast to observations reported previously when cuprous ion was added to bleomycin (Dabrowiak et al., 1978), the addition of either ferrous or ferric iron to bleomycin A_2 had no effect on the position of the bleomycin A_2 peak at 288 nm in 0.1 M succinate at pH 6.2 (data not shown).

Titrations of bleomycin with either ferrous or ferric iron show an initial rapid increase in optical activity of the bleomycin complex. In both cases, saturation occurs sharply at a bleomycin/iron ratio of 1:1. The extinction coefficients that we calculate for the ferrous and ferric iron–bleomycin complexes in 0.1 M succinate at pH 6.2 are E^{460} = 0.225 OD/mM and E^{430} = 1.775 OD/mM, respectively.

The product of the reaction between ferrous iron and bleomycin A_2 is a ferric iron–bleomycin complex (Caspary et al., 1979; Sausville et al., 1978a,b). In the buffers used, this complex can exist in two forms that are readily distinguishable by their ESR spectra (Figure 4). The high-spin rhombic form of the ferric iron–bleomycin complex is characterized by an ESR peak at g = 4.3. The low-spin form manifests an ESR spectrum possessing three peaks with g values of 2.40, 2.17, and 1.89 (Sugiura & Kikuchi, 1978). There appear to be no

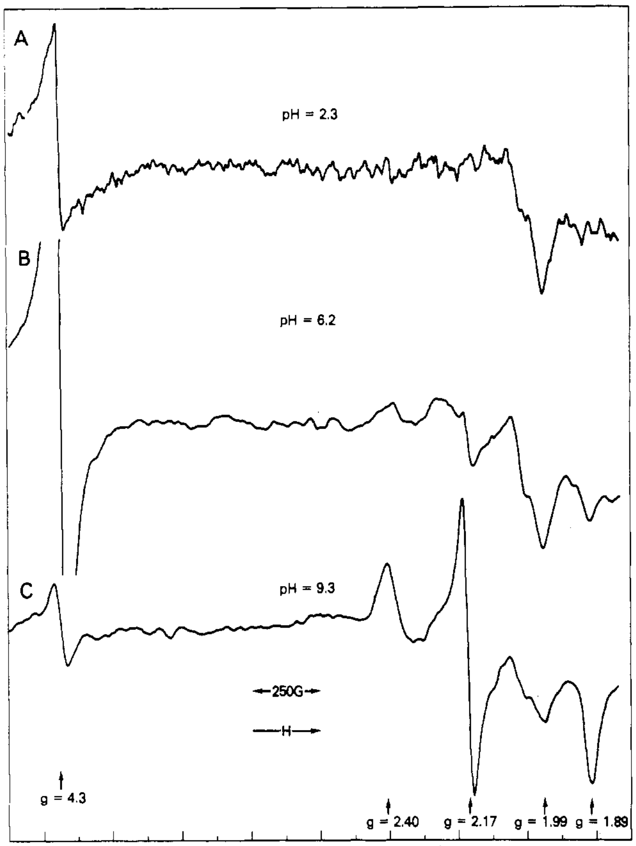

FIGURE 4: ESR spectra of the ferric iron–bleomycin complex. Solutions of 6×10^{-3} M bleomycin and 10^{-4} M ferric iron were prepared in (A) 0.1 M glycine–HCl, pH 2.3, (B) 0.1 M maleate, pH 6.2, and (C) 0.1 M glycine–KOH, pH 9.3. When ferrous iron was used instead of ferric iron, the spectra were similar except that, at pH 2.3, no ESR peaks were observed. Conditions under which ESR spectra were obtained are described under Materials and Methods.

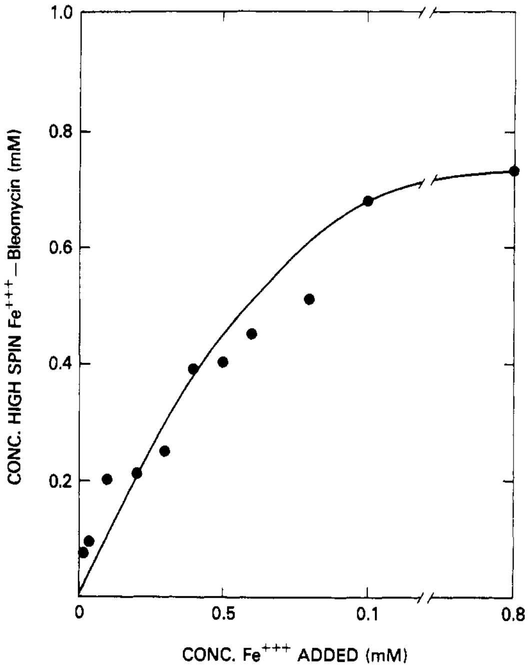

FIGURE 5: Titration of bleomycin by ferric iron monitored by the ESR spectra of the high-spin ferric iron–bleomycin complex. Increasing concentrations of ferric iron were added to 0.11 mM bleomycin at pH 6.2 in 0.1 M maleate. ESR spectra of controls containing iron at equivalent concentrations and without bleomycin were run. No ESR spectra were observed. Concentrations of the high-spin ferric iron–bleomycin complex were determined by double integration of the $g = 4.3$ signal. Comparing double-integral values of the $g = 4.3$ signal with that of the low-spin signal indicates that 80% of the iron–bleomycin complex is in the high-spin state. Since the concentration of bleomycin A_2 added was 1.1×10^{-4} M, the effective total concentration available in the high-spin complex is 0.88×10^{-4} M, indicating that a 1:1 high-spin ferric iron–bleomycin complex is formed.

peaks outside this range. The peak at $g = 1.99$ is present in all our spectra and has not been identified. It appears to be an impurity in the system. The ESR spectra of the ferric iron–bleomycin complex produced by adding ferric or ferrous iron to bleomycin in air are similar except at pH 2.3. At this pH, the addition of ferrous iron to bleomycin results in no ESR spectrum since very little, if any, oxygen is consumed (Table I) and, hence, no ferric iron is formed.

The relative concentrations of high-spin and low-spin forms are pH dependent. When ferric iron (final concentrations 10^{-4} M) is added to bleomycin (final concentration 6×10^{-3} M) at pH 2.3 in glycine–HCl, a peak at $g = 4.3$ is seen (Figure 4A). No low-spin ferric iron complex is observed even at the high gains used. Ferric iron (10^{-4} M), in the absence of bleomycin, is refractory to ESR measurements. By increasing the pH to 6.2 and 9.3, the ratio of concentrations of the low-spin form to high-spin form increases (Figure 4B,C). The relative concentrations of the two forms can be reversibly changed by adjusting the pH. Thus, when HCl is added to a ferric iron–bleomycin solution at pH 9.3 to form a solution at pH 2.3 or when KOH is added to a ferric iron–bleomycin solution at pH 2.3 to form a solution at pH 9.3, the resulting ESR spectra are characteristic of the spectra shown in Figure 4, parts A and C, respectively. This suggests that the ligand structure surrounding the ferric iron is affected by pH. At pH 6.2 in maleate, approximately 80% of the ferric iron is in the high-spin form as measured by double integration of the ESR spectrum.

The saturation curve shown in Figure 5 demonstrates the binding between high-spin ferric iron and bleomycin at pH 6.2. At this pH, approximately 80% of the ferric iron is in the high-spin form. Since the concentration of the high-spin complex asymptotically approaches 0.8 mM (or approximately 80% of the bleomycin A_2 added), this graph demonstrates that high-spin ferric iron and bleomycin form a 1:1 complex.

The ESR spectrum of the product of the reaction between ferrous iron and bleomycin in air is obtained by freezing the solution 60 s after being mixed (Figure 6A) and is composed of the high-spin and low-spin contributions. These solutions were prepared at pH 9.3 since at this pH the bleomycin-induced rate of oxygen uptake is high (Table I).

If the solution is frozen 5 s after ferrous iron is mixed with bleomycin, a transient low-spin ferric complex characterized by ESR peaks at $g = 2.24$, 2.17, and 1.93 (Figure 6B) is trapped. The ESR spectrum of the transient species (Figure 6B), like that of the ferric iron–bleomycin complex, does not saturate at 200 mW. This is characteristic of the ESR spectra of paramagnetic metal ions. Since the three-line spectrum is characteristic of low-spin ferric iron, the transient species could be a ternary complex of unknown structure composed of ferric iron, superoxide radical, and bleomycin. When potassium superoxide is added to bleomycin, no ESR spectrum is observed except that characteristic of the superoxide radical (Figure 6D).

To characterize this transient species further, we added 0.1 mg of solid $KO_2\cdot$ to 1 mL of a buffered solution containing the ferric iron–bleomycin complex which was formed by the addition of either ferrous or ferric iron to bleomycin. When this solution was quickly frozen in liquid N_2 5 s after mixing, the ESR spectrum manifested peaks at $g = 2.24$, 2.17, and

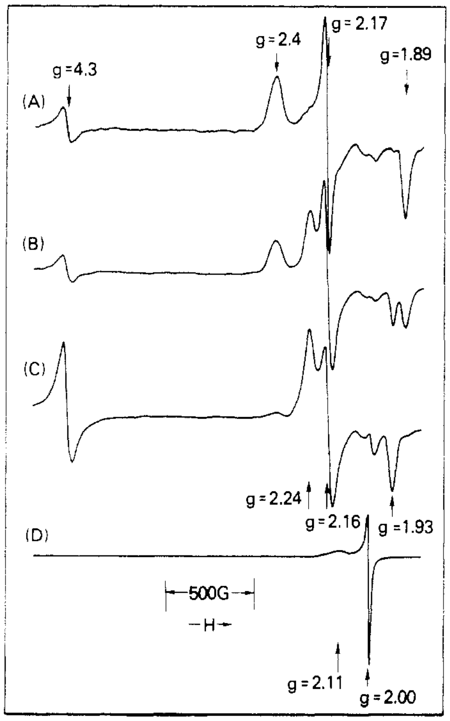

FIGURE 6: ESR spectra of the iron–bleomycin–oxygen intermediate. Solutions of 6×10^{-3} M bleomycin and 10^{-4} M ferrous or ferric iron were prepared in 0.1 M glycine–KOH at pH 9.3 (final pH). Solutions were placed into ESR tubes and frozen in liquid N_2. (A) The ESR spectrum of a solution of ferrous iron added to bleomycin and frozen after 60 s. (B) The ESR spectrum of a solution of ferrous iron added to bleomycin and frozen after 5 s. (C) The ESR spectrum of the ferric iron–bleomycin complex after 0.1 μg of solid $KO_2\cdot$ is added and the resultant solution is frozen in liquid N_2 5 s after addition of $KO_2\cdot$. (D) ESR spectrum of $KO_2\cdot$ at pH 9.3 produced by the addition of excess $KO_2\cdot$ to bleomycin. Conditions under which the ESR spectra were obtained are presented under Materials and Methods.

1.93 (Figure 6C). This spectrum is characteristic of ferric iron in a low-spin state and is identical with the transient species observed when ferrous iron is added to bleomycin in air (Figure 6B). This complex is converted back to the ferric iron–bleomycin product upon standing in air.

The superoxide radical can, under appropriate conditions, act as a reducing agent. However, our evidence indicates that it is unable to reduce the ferric iron–bleomycin complex to the ferrous state. We examined the color of iron solutions in the presence of 2,2′-bipyridine, which is red in the presence of ferrous iron (Table III). These reactions were performed under nitrogen in 0.1 M glycine–KOH (pH 9.3) and in air in 0.1 M maleate (pH 6.2) and in 0.1 M glycine–HCl (pH 3.4). The addition of potassium superoxide did not change the pH by more than 0.2 unit.

At pH 9.3 under nitrogen, if ferrous iron is replaced by 0.1 mM ferric iron in the absence of bleomycin, the color of the solution changes from red to colorless. In the presence of bleomycin and under nitrogen, the addition of ferrous iron causes a dark pink color to appear. The addition of potassium superoxide to a ferric iron–bleomycin complex does not turn the solution pink, indicating that either ferrous iron is not formed or, if it is, it is reoxidized back to the ferric state by H_2O_2 formed by the decomposition of the superoxide radical. We ruled out this latter possibility by adding catalase to the solution and observing that the solution did not turn pink.

At pH 6.2 in the presence of 2,2′-bipyridine, ferrous sulfate turns the solution dark red since autoxidation is inhibited (Table I). If 0.2 mM bleomycin is present, the addition of 0.1 mM ferrous sulfate does not turn the solution red since the ferrous iron is oxidized to the ferric state. When potassium superoxide was added to a solution containing ferric iron and bleomycin, no red color was observed.

Table III: Effect of Superoxide Radical on Iron Solution in the Presence of 2,2′-Bipyridine[a]

pH	bleo-mycin	Fe^{3+}	Fe^{2+}	N_2	catalase	$O_2\cdot$	color
9.3	–	+	–	+	–	–	colorless
9.3	–	–	+	+	–	–	red
9.3	+	–	+	+	–	–	dark pink
9.3	+	+	–	+	+	+	pale yellow
6.2	–	–	+	–	–	–	red
6.2	–	+	–	–	–	–	colorless
6.2	+	–	+	–	–	–	pale yellow
6.2	–	+	–	–	–	+	colorless
6.2	–	+	–	–	+	+	colorless
6.2	+	+	–	–	+	+	pale yellow
3.4	+	–	+	–	–	–	red
3.4	+	+	–	–	+	+	colorless

[a] The final concentrations were 0.1 mM ferrous or ferric iron, 0.2 mM bleomycin, 18–20 μg/mL catalase, and 0.1 M glycine–KOH (pH 9.3), 0.1 M maleate (pH 6.2), or 0.1 M glycine–HCl (pH 3.4). The addition of 10 mM potassium superoxide did not increase the pH of any of these solutions by more that 0.2 pH unit. At pH 6.2, the autoxidation of ferrous iron occurs spontaneously. At pH 6.2, ferrous iron is oxidized only in the presence of bleomycin. At pH 3.4, ferrous ion autoxidation is inhibited even in the presence of bleomycin. Catalase is added to prevent the reoxidation of ferrous iron by a reaction with H_2O_2 formed by the decomposition of the superoxide radical.

In a similar experiment in air at pH 3.4 where the ferrous iron–bleomycin complex does not autoxidize in the presence of oxygen (Table I), the addition of 0.1 mM ferrous iron and 0.2 mM bleomycin turned the solution dark red. However, the addition of potassium superoxide to the ferric iron–bleomycin complex did not turn the solution red.

Thus, at all three conditions, a red color is formed in the presence of 2,2′-bipyridine and ferrous iron unless the ferrous iron is oxidized to the ferric state. When 0.1 mM ferric iron is added to a solution of bleomycin and 2,2′-bipyridine, the solution is clear. When 10 nM potassium superoxide is added to 0.1 mM ferric iron in the presence or absence of bleomycin at any of these pHs, the color remains clear.

These experiments indicate that potassium superoxide is unable to reduce a ferric iron–bleomycin complex to the ferrous state. Because of this and because the ESR spectrum is characteristic of a low-spin ferric iron, the transient species shown in Figure 6B cannot be a ferrous complex.

If potassium superoxide is unable to reduce the ferric iron–bleomycin complex to the ferrous state, then the question of how this reduction takes place in the cell must be addressed. Glutathione, a reducing agent containing a sulfhydryl group, is able to reduce the ferric iron in the ferric iron–bleomycin complex. The ESR spectrum of the ferric iron–bleomycin complex (Figure 7A), which was frozen for ESR observations, changed to a low-spin ferric complex with *g* values of 2.32, 2.19, and 1.93 (Figure 7B) when 10^{-3} M glutathione was added. After approximately 0.5 h at room temperature, these signals totally disappeared (Figure 7C). When the solution was then bubbled with oxygen and refrozen, the ESR spectrum characteristic of the ferric iron–bleomycin complex returned. Concurrently, a solution of 2,2′-bipyridine was added to an aliquot of the ferric iron–bleomycin complex. Over the 0.5-h period, the color gradually changed from colorless to pink. The pink color and the concurrent disappearance of the ESR spectrum indicate that after 0.5 h the ferric iron is reduced to the ferrous state. In the absence of bleomycin, glutathione

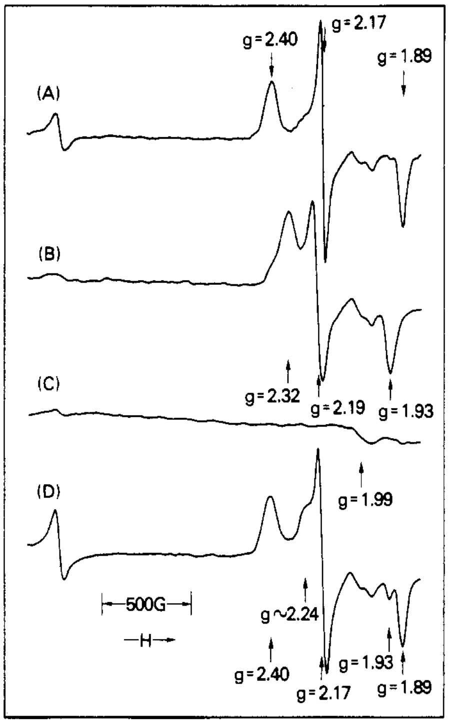

FIGURE 7: ESR spectra of a glutathione–ferric iron–bleomycin complex. (A) Spectrum of 10^{-4} M ferric iron and 6×10^{-3} M bleomycin in glycine–KOH at pH 9.3. (B) Spectrum of 10^{-4} M ferric iron, 6×10^{-3} M bleomycin, and 5×10^{-4} M glutathione frozen in liquid N_2 1 min after the addition of glutathione. (C) Spectrum of 10^{-4} M ferric iron, 6×10^{-3} M bleomycin, and 5×10^{-4} M glutathione frozen in liquid N_2 30 min after the addition of glutathione. (D) Spectrum of 10^{-4} M ferric iron, 6×10^{-3} M bleomycin, and 5×10^{-4} M glutathione incubated for 30 min before being aerated. Conditions under which the ESR spectra were obtained are presented under Materials and Methods.

immediately turns a ferric iron solution pink in the presence of 2,2′-bipyridine. No ESR spectrum is observed when glutathione is added to a solution of ferric iron in the absence of bleomycin. The ESR peak at $g = 4.3$ due to the ferric iron–bleomycin complex was not affected during the first 0.5 h after addition of glutathione. After 0.5 h, this signal disappeared. It re-formed after the solution was bubbled with oxygen.

Discussion

We have previously proposed that bleomycin acts like a ferrous oxidase to reduce oxygen catalytically and to form active, reduced oxygen species including $O_2\cdot$, H_2O_2, and $OH\cdot$ (Figure 2). In acidic solutions (pH less than 5), no reaction occurs. Above pH 5, the difference between oxygen consumption induced by ferrous iron and that induced in the presence of ferrous iron and bleomycin is relatively constant. Identifying oxygen consumption induced by the ferrous iron–bleomycin complex with this difference implies that the presence of bleomycin in the reaction mixture has little effect on the mechanism of spontaneous ferrous iron autoxidation. Since the validity of this assumption is unknown, we chose to do most of our kinetic work in maleate at pH 6.2 where the spontaneous rate of 10^{-4} M ferrous iron autoxidation is 0 (Caspary et al., 1979).

The effect of chelating agents on oxygen consumption induced by bleomycin would be expected to depend on the ability of the particular chelating agent to compete with bleomycin in binding ferrous iron. It appears that all three chelating agents tested (EDTA, *o*-phenanthroline, and 2,2′-bipyridine) effectively compete with bleomycin for the ferrous iron. The nature of the resultant complex appears to determine its ability to induce oxygen consumption since it is totally inhibited in the presence of 2,2′-bipyridine and *o*-phenanthroline and is stimulated in the presence of EDTA.

The first species in the ferrous oxidase cycle of bleomycin in air is the ferrous iron–bleomycin complex which can be considered to be the enzyme–substrate complex (Caspary et al., 1979; Sausville et al., 1976). The product of the reaction is a ferric iron–bleomycin complex (Caspary et al., 1979; Sausville et al., 1976, 1978a,b). At pH 6.2, it forms a 1:1 complex with bleomycin. This complex exists in at least two forms, which agrees with the results of Burger et al. (1979a) published after this work was submitted. The low-spin form possesses less than axial symmetry as evidenced by the different values for the principal component of the **g** tensor. The absence of axial symmetry for both the high- and low-spin forms is probably due to the flexible and unsymmetric nature of the ferric iron–bleomycin complex.

The interconvertibility between these two forms that we observe as a function of pH is similar to effects on microsomal Fe_x reported by Murakami & Mason (1967). These authors reported an increasing ESR signal at $g = 6$, which they attributed to the high-spin form, and the concomitant decrease in low-spin signals with increasing pH, a phenomenon similar to our observations with the ferric iron–bleomycin complex. Murakami and Mason attributed their results to changes in one or more of the iron binding sites as a function of pH and concluded that at least one of the binding sites is labile. The high-spin form of the ferric iron–bleomycin complex possesses an ESR spectrum at $g = 4.3$, characteristic of high-spin ferric iron in a rhombic conformation.

The difference between the high-spin and low-spin forms of ferric iron essentially lies in the accessibility of the e_g orbitals ($d_{x^2-y^2}$ and d_{z^2}) to the five d electrons. The energy separation between the e_g and t_{2g} (d_{xy}, d_{yz}, and d_{xz}) orbitals is a function of the distorted octahedral crystal field produced by the ligands. Any change in the molecular environment causing modification or lability of the ligands (e.g., substitution or protonation) can change the energy separation. If the energy separation is decreased, the high-spin form will be more favored since thermal energy will cause the electron population of the e_g orbitals to increase as predicted by the Boltzmann distribution. Strong ligand fields manifest themselves as the low-spin forms of the ferric iron.

Our inability to observe a decrease in the initial rate of oxygen uptake by superoxide dismutase in the presence of bleomycin (Table II) may be due to an immediate dismutation of the newly formed superoxide radical in the absence of SOD (Mason et al., 1978) or to a relative stability of a bleomycin–iron–oxygen complex. If rapid dismutation were the reason, the addition of catalase should have an effect on the rate of oxygen consumption unless the hydrogen peroxide formed from the superoxide radical were extremely unstable due to its reaction with ferrous iron. While hydrogen peroxide reacts with ferrous salts [$k = 76$ M^{-1} s^{-1} (Schonbaum & Chance, 1976)], its decomposition in the presence of catalase is half a million times faster [$k = 4 \times 10^7$ M^{-1} s^{-1} (Wilshire & Sawyer, 1979)]. Experimentally, we show that in the absence of bleomycin, catalase inhibits oxygen consumption in the presence of ferrous salts (Table II) and inhibits ethylene formation from methional (W. J. Caspary, unpublished data), indicating that ferrous iron cannot compete with catalase for hydrogen peroxide. Thus, the absence of an effect on oxygen uptake upon the addition of catalase (Table II) suggests that superoxide dismutation is delayed. A time delay in releasing the superoxide radical into the medium would impede this radical's accessibility to superoxide dismutase. This time delay could be caused by the formation of a relatively stable complex. Thus, at any time point, small amounts of oxygen would be re-formed compared to the amount of oxygen already consumed. Since the amount of oxygen re-formed is half the amount of superoxide radical released, detection of the apparent inhibition could be difficult.

The possibility that there might be a relatively stable intermediate caused us to search for such a species by ESR. The appearance of an ESR signal with $g = 2.24$, 2.17, and 1.93 suggested that a transient species may exist. This same intermediate is formed when $KO_2\cdot$ is added to the ferric iron–bleomycin complex. The simplest explanation for these data is that this intermediate is composed of bleomycin, ferric iron, and superoxide ion.

The exact location of this oxygen species with respect to the iron and bleomycin moieties in this proposed intermediate cannot be determined from these data. The reaction proceeds as a dynamic event. Initially, the oxygen approaches the ferrous iron–bleomycin complex. When in close proximity, an electron is transferred from the iron to the oxygen. The oxygen species is then released. The species trapped and observed by ESR could be any structure formed after electron transfer and before the complete release of the oxygen radical into the medium. The same species is observed when the superoxide radical is added to the ferric iron–bleomycin complex. The ESR spectrum of the ferric iron–bleomycin complex is re-formed after the intermediate is allowed to sit at room temperature for 5 min. This indicates that this reaction is reversible and suggests that $O_2^-\cdot$ binds to a labile site on the bleomycin–iron complex and does not react with the bleomycin molecule. The inability to saturate these ESR signals at 200 mW and the absence of an ESR signal when potassium superoxide is added to bleomycin in the absence of iron provide further evidence that the ESR signal observed is due to a ferric iron complex and not a radical species produced by a reaction of the superoxide radical with bleomycin. The superoxide radical does not appear to lose its identity though its relaxation time may change when near the paramagnetic ferric iron. Because of the transient species' unique ESR spectrum, the oxygen species must either directly influence the ferric ligand field or modify the bleomycin binding to this metal ion. It should be emphasized that although the inability to inhibit oxygen uptake by SOD suggests a relatively stable intermediate, our evidence does not prove that the proposed intermediate inhibiting the effect of superoxide dismutase is necessarily identical with the transient species observed by ESR.

An oxygenated form of cytochrome P-450 was reported by Ishimura et al. (1971). This species was observed optically by adding oxygen to the ferrous form of bacterial cytochrome P-450. While the ferric product of this enzyme produced the characteristic low-spin ESR signal, no such signal could be associated with this oxygenated intermediate species. On the basis of this evidence, the authors ascribed this species to be a ferrous iron–oxygen–cytochrome P-450 intermediate. The authors did not discuss the possibility of transferring the electron from the ferrous iron to the oxygen. Such a possibility is discussed by Strobel & Coon (1971) who reported that a superoxide radical is produced in a reconstituted system of cytochrome P-450, TPNH, cytochrome P-450 reductase, and phosphatidylcholine hydroxylated benzphetamine. It appears that the stability of the complexes formed between ferrous and ferric iron and oxygen is a function of the ligand structure of the entire complex. In a report that appeared after the submission of this paper, Burger et al. (1979b) reported evidence for a ferrous iron–oxygen bleomycin complex. Their work was done at pH 5.5 in the absence of buffer. Since the addition of ferrous iron to a nonbuffered solution tends over a 2-h period to decrease the pH and since at a pH below 5 or 6 oxygen consumption is inhibited (Table I), it is unclear whether such a stable complex is important in the consumption of oxygen. At pH 9.3 where the ESR spectrum of the transient species is observed, oxygen reduction proceeds rapidly. However, the reaction must proceed through a ferrous–oxygen–bleomycin structure. The stabilities of these intermediates may well be a function of pH. If any form of an iron–oxygen–bleomycin complex were too stable, oxygen consumption would be inhibited.

Both glutathione and the superoxide radical, when added to the ferric iron–bleomycin complex, shift the ESR peaks in the low-spin region of the spectrum. They do not change the general low-spin signature of the resulting complexes. This suggests that these compounds associate with the ferric iron–bleomycin complex but do not, at least initially, change its general ESR characteristics. After the association occurs, glutathione, unlike the superoxide radical, is able to reduce ferric iron in the complex, as evidenced by the disappearance of the ESR spectrum and by the solution turning red in the presence of 2,2′-bipyridine. This reduction by glutathione is not accompanied by a destruction of the iron–bleomycin complex since the process is reversible when air is introduced to the reduced complex. In contrast to this, the superoxide radical associates with the ferric iron–bleomycin complex, but is unable to reduce it. Rather, it rapidly dissociates from the complex to form the ferric iron–bleomycin complex.

The ability of glutathione to reduce the ferric iron–bleomycin complex to the ferrous state may serve as a model for the biological reduction of the ferric iron–bleomycin complex (Figure 2). However, since glutathione also reduces ferric iron in the absence of bleomycin, we cannot determine whether ferric iron is reduced when actually bound to the bleomycin. However, since the addition of ferric iron to bleomycin causes broadening of certain lines of the carbon-13 bleomycin NMR spectrum (Gupta et al., 1979), the exchange rate describing the iron binding must be greater than 10^3/s. The reaction of bleomycin and ferrous iron follows Michaelis–Menten kinetics (Caspary et al., 1979), an experiment that was performed in the absence of an organic reducing agent but in the presence of excess ferrous iron. We anticipate that because iron binding to bleomycin undergoes an exchange process, ferrous iron can replace a ferric iron to continue the catalytic cycle. The presence of reducing agents in the cell such as sulfhydryl groups, ascorbic acid, and NADPH adds credibility to the possibility of this mechanism. Free ferric iron either dissociated from the bleomycin or obtained elsewhere may be the actual species reduced.

Acknowledgments

We are indebted to Rosalind Friedman for her skilled technical assistance and Dr. Stephen Lesko for his advice after reading the manuscript.

References

Bearden, J., Jr., & Haidle, C. W. (1975) *Biochem. Biophys. Res. Commun. 65*, 371.

Bearden, J. C., Lloyd, R. S., & Haidle, C. W. (1977) *Biochem. Biophys. Res. Commun. 75*, 442.

Beauchamp, C., & Fridovich, I. (1970) *J. Biol. Chem. 245*, 4641.

Burger, R., Peisach, J., Blumberg, W., & Horwitz, S. (1979a) *J. Biol. Chem. 254*, 10906.

Biochemistry **1981**, *20*, 3875–3879

Burger, R., Horwitz, S., Peisach, J., & Wittenberg, J. (1979b) *J. Biol. Chem. 254*, 12299.

Caspary, W. J., Lanzo, D. A., Niziak, C., Friedman, R., & Bachur, N. R. (1979) *Mol. Pharmacol. 16*, 256.

Dabrowiak, J. C., Greenaway, F. T., Lonzo, W. E., Van Husen, M., & Crooke, S. T. (1978) *Biochim. Biophys. Acta 517*, 517.

Gupta, R., Ferretti, J., & Caspary, W. (1979) *Biochem. Biophys. Res. Commun. 89*, 534.

Haidle, C. (1971) *Mol. Pharmacol. 7*, 645.

Haidle, C. W., Weiss, K. K., & Kuo, M. T. (1972) *Mol. Pharmacol. 8*, 531.

Iqbal, Z. M., Kohn, K. W., Ewig, R. A., & Fornace, A. J., Jr. (1976) *Cancer Res. 36*, 3834.

Kohn, K. W., & Ewig, R. A. (1976) *Cancer Res. 36*, 3839.

Kuo, M. T., Haidle, C. W., & Inners, L. D. (1973) *Biophys. J. 13*, 1296.

Lloyd, R. S., Haidle, C. W., & Robberson, D. L. (1978) *Biochemistry 17*, 1890.

Lown, J. W., & Sim, S. K. (1977) *Biochem. Biophys. Res. Commun. 77*, 1150.

Mason, R., Peterson, F., & Holtzman, J. (1978) *Mol. Pharmacol. 14*, 665.

Murakami, K., & Mason, H. S. (1967) *J. Biol. Chem. 242*, 1102.

Naganawa, H., Muraoka, Y., Takita, T., & Umezawa, H. (1977) *J. Antibiot. 30*, 388.

Sausville, E. A., Peisach, J., & Horwitz, S. B. (1976) *Biochem. Biophys. Res. Commun. 73*, 814.

Sausville, E. A., Peisach, J., & Horwitz, S. B. (1978a) *Biochemistry 17*, 2740.

Sausville, E. A., Stein, R. W., Peisach, J., & Horwitz, S. B. (1978b) *Biochemistry 17*, 2746.

Schonbaum, G., & Chance, B. (1976) *Enzymes, 3rd Ed.*, 363.

Sugiura, Y., & Kikuchi, T. (1978) *J. Antibiot. 31*, 1310.

Suzuki, H., Nagai, K., Yamaki, H., Tanaka, N., & Umezawa, H. (1969) *J. Antibiot. 22*, 446.

Takeshita, M., Horwitz, S. B., & Grollman, A. P. (1974) *Virology 60*, 455.

Takeshita, M., Grollman, A., & Horwitz, S. B. (1976) *Virology 69*, 453.

Umezawa, H., Maeda, K., Takeuchi, T., & Okami, Y. (1966a) *J. Antibiot., Ser. A 19*, 200.

Umezawa, H., Suhara, Y., Takita, T., & Maeda, K. (1966b) *J. Antibiot., Ser. A 19*, 210.

Wilshire, J., & Sawyer, D. (1979) *Acc. Chem. Res. 12*, 105.

Isolation and Identification of 23,25-Dihydroxyvitamin D_3, an in Vivo Metabolite of Vitamin D_3[†]

Yoko Tanaka, Joseph K. Wichmann, Heinrich K. Schnoes, and Hector F. DeLuca*

ABSTRACT: Vitamin D supplemented rats produce a metabolite of 25-hydroxy[3α-^{3}H]vitamin D_3 that is easily separated from known metabolites by using high-performance liquid chromatography. The production of this metabolite in vivo as well as 1,25-dihydroxyvitamin D_3, 24(*R*),25-dihydroxyvitamin D_3, and 25-hydroxyvitamin D_3 26,23-lactone is largely if not totally eliminated by nephrectomy. Kidney homogenates from vitamin D supplemented chickens incubated with 25-hydroxyvitamin D_3 produce significant quantities of the new, unknown metabolite. This metabolite was isolated in pure form from such incubation mixtures by using both straight-phase and reversed-phase high-performance liquid chromatography. This metabolite has been positively identified as 23,25-dihydroxyvitamin D_3 by ultraviolet absorption spectrophotometry, mass spectrometry, and derivatization. This structure was confirmed by chemical synthesis of both C-23 stereoisomers. Although the natural product exactly comigrates with one of the synthetic isomers, the exact stereochemistry of the natural product remains unknown. It is possible that this new metabolite is an intermediate in the biosynthesis of 25-hydroxyvitamin D_3 26,23-lactone.

In the past 15 years significant progress has been made in our understanding of the metabolism of vitamin D_3 (DeLuca, 1979, 1980). However, much remains to be learned in this area since it is not yet possible to describe the total pathway of metabolism of this important vitamin. Recently, a major metabolite of vitamin D_3 has been found in the plasma of animals and man (Horst et al., 1979; Shepard & DeLuca, 1980). This compound has been isolated in pure form and its structure unequivocally demonstrated to be 25-hydroxyvitamin D_3 26,23-lactone (25-OH-D_3-26,23-lactone)[1] (Wichmann et al., 1979). This structure has recently been confirmed by chemical synthesis (Wichmann et al., 1980). The unexpected structure of this compound has fostered a significant effort to elucidate its pathway of biosynthesis (Tanaka et al., 1980; Littledike et al., 1980). Nephrectomy eliminates biosynthesis of the 25-OH-D_3-26,23-lactone (Tanaka et al., 1980; Littledike et al., 1980). Homogenates of kidney tissue prepared from chickens given large doses of vitamin D_3 are able to convert 25-hydroxyvitamin D_3 (25-OH-D_3) to the 25-OH-D_3-26,23-

---

[†] From the Department of Biochemistry, College of Agricultural and Life Sciences, University of Wisconsin—Madison, Madison, Wisconsin 53706. *Received November 25, 1980.* This work was supported by National Institutes of Health Program-Project Grant AM-14881 and the Harry Steenbock Research Fund of the Wisconsin Alumni Research Foundation.

[1] Abbreviations used: 25-OH-D_3-26,23-lactone, 25-hydroxyvitamin D_3 26,23-lactone; HPLC, high-performance liquid chromatography; 25-OH-D_3, 25-hydroxyvitamin D_3; 1,25-$(OH)_2D_3$, 1,25-dihydroxyvitamin D_3; 24(*R*),25-$(OH)_2D_3$, 24(*R*),25-dihydroxyvitamin D_3; 25,26-$(OH)_2D_3$, 25,26-dihydroxyvitamin D_3; 23,25-$(OH)_2D_3$, 23,25-dihydroxyvitamin D_3; ATP, adenosine 5′-triphosphate; NADP, nicotinamide adenine dinucleotide.

0006-2960/81/0420-3875$01.25/0